Available online at www.sciencedirect.com
ScienceDirect
Advances in Space Research 41 (2008) 2050–2055
ADVANCES IN SPACE RESEARCH
(a COSPAR publication)
www.elsevier.com/locate/asr

Search for fractionally charged particles in cosmic rays with the BESS spectrometer

H. Fuke [a,*], Y. Tasaki [a], K. Abe [b,1], S. Haino [c,2], Y. Makida [c], S. Matsuda [c], J.W. Mitchell [d], A.A. Moiseev [d], J. Nishimura [e], M. Nozaki [c], S. Orito [e,✠], J.F. Ormes [d,3], M. Sasaki [d], E.S. Seo [f], Y. Shikaze [b,4], R.E. Streitmatter [d], J. Suzuki [c], K. Tanaka [c], T. Yamagami [a], A. Yamamoto [c], T. Yoshida [a], K. Yoshimura [c]

[a] *Institute of Space and Astronautical Science, Japan Aerospace Exploration Agency (ISAS/JAXA), Sagamihara, Kanagawa 229-8510, Japan*
[b] *Kobe University, Kobe, Hyogo 657-8501, Japan*
[c] *High Energy Accelerator Research Organization (KEK), Tsukuba, Ibaraki 305-0801, Japan*
[d] *National Aeronautics and Space Administration, Goddard Space Flight Center (NASA/GSFC), Greenbelt, MD 20771, USA*
[e] *The University of Tokyo, Tokyo 113-0033, Japan*
[f] *University of Maryland, College Park, MD 20742, USA*

Received 11 November 2006; received in revised form 24 January 2007; accepted 13 February 2007

Abstract

Historically, there are been many searches for fractionally charged particles in the cosmic radiation. However, few searches have been performed near the top of the atmosphere. We performed a search for relativistic $\frac{2}{3}e$ charged particles in cosmic rays using data collected during four BESS balloon flights from 1997 to 2000 carried out in northern Canada. The data were analyzed by examining energy deposition in the time-of-flight scintillator hodoscopes. No candidate was found. We derive an upper limit of 4.5×10^{-7} (cm^2 s sr)$^{-1}$ for the flux of $\frac{2}{3}e$ charged particles, at the 90% confidence level.

Keywords: Cosmic ray; Fractional charge; Quark search; Superconducting spectrometer; BESS

1. Introduction

The origin of the electric charge quantization is a fundamental question for elementary particle physics, but it remains unexplained within the Standard Model. Since the proposal of the quark model in 1964, many searches for fractionally charged particles have been carried out in the cosmic radiation without any evidence for their existence. However, most of these searches were performed on or under ground on the assumption that the objective particles are able to penetrate large amount of material (Table 1). Therefore, it is worthwhile to do a search near the top of the atmosphere where there is around 5 g/cm^2 of intervening material.

Here, we report a search for relativistic $\frac{2}{3}e$ charged particles in cosmic rays using the data collected during four BESS balloon flights from 1997 to 2000 carried out in northern Canada.

2. BESS spectrometer

The BESS detector (Fig. 1) was designed (Orito, 1987; Yamamoto et al., 1988) and developed (Ajima et al.,

* Corresponding author.
E-mail address: fuke@balloon.isas.jaxa.jp (H. Fuke).
[1] Present address: Kamioka Observatory, ICRR, The University of Tokyo, Kamioka-cho, Gifu 506-1205, Japan.
[2] Present address: Istituto Nazionale di Fisica Nucleare (INFN), Universita degli Studi di Perugia, Perugia 06123, Italy.
[3] Present address: University of Denver, Denver, CO 80208, USA.
[4] Present address: Tokai Research Establishment, Japan Atomic Energy Research Institute (JAERI), Tokai, Ibaraki 391-1195, Japan.
✠ Deceased.

0273-1177/$34.00 © 2007 COSPAR. Published by Elsevier Ltd. All rights reserved.
doi:10.1016/j.asr.2007.02.042

Table 1
Examples of searches for fractionally charged particles in cosmic radiation

Reference	Objects	Upper limit (cm^{-2} s^{-1} sr^{-1})
In primary cosmic rays		
Sbarra et al. (2002)	$\frac{2}{3}e$	3.0×10^{-7} (95% C.L.) (preliminary)
On the mountain		
DeLise and Bowen (2004)	$\frac{1}{3}e$, $\frac{2}{3}e$	1.8×10^{-8} (90% C.L.) ($\frac{2}{3}e$)
On or under ground		
Ambrosio et al. (2004) and Ambrosio et al. (2000)	$\frac{1}{5}e - \frac{2}{3}e$	6.1×10^{-16} (90% C.L.) ($0.25 < \beta < 1$)
Aglietta et al. (1994)	$\frac{1}{3}e$, $\frac{2}{3}e$	2.7×10^{-13} (90% C.L.) ($\frac{2}{3}e$)
Mori et al. (1991)	$\frac{1}{3}e$, $\frac{2}{3}e$	2.3×10^{-15} (90% C.L.) ($\frac{2}{3}e$)
Mashimo et al. (1983) and Kawagoe et al. (1984)	$\frac{1}{3}e$, $\frac{2}{3}e$	6×10^{-13} (90% C.L.) ($\frac{2}{3}e$, $3.5 \times 10^{-4} < \beta < 0.4$)

2000; Makida et al., 1995; Shikaze et al., 2000; Asaoka et al., 1998) as a high-resolution spectrometer with the large geometrical acceptance and strong particle-identification capability. A uniform magnetic field of one Tesla is generated by a thin superconducting solenoid. The field region is filled with tracking detectors consisting of a jet-type drift chamber (JET) and two inner drift chambers (IDCs). Tracking is performed by fitting up to 28 hit points in these drift chambers, resulting in a rigidity (R) resolution of 0.5% at one GV. The upper and lower time-of-flight scintillator hodoscopes (TOFs) measure the velocity (β) and the energy loss (dE/dx). The time resolution of each counter is 55 ps, which yields a $1/\beta$ resolution of 1.4%.

3. Balloon flights

Four balloon flights were carried out in northern Canada, 1997 through 2000. They flew from Lynn Lake to Peace River where the geomagnetic cutoff rigidity ranges from 0.3 to 0.5 GV. Data for the search were taken for live times of 15.8, 16.8, 27.4, and 28.7 h in 1997, 1998, 1999, and 2000, respectively, at altitudes around 36 km, corresponding to $\sim$5 g/cm^2 in residual atmospheric depth. The data acquisition sequence was initiated by a first-level trigger generated by a coincidence between hits of the upper and lower TOFs with a threshold set at $\frac{1}{3}$ of the pulse height from minimum ionizing particles (MIPs). In addition to biased trigger modes enriching negatively charged particles, one of every 60 (30 in 2000) first-level triggered events were recorded as unbiased samples (Ajima et al., 2000).

4. Data analysis

The unbiased samples were used to search for $\frac{2}{3}e$ charged particles. As described later, the "key" information to identify $\frac{2}{3}e$ particles is the energy deposit measured by the upper and lower TOFs. The typical energy loss of relativistic $\frac{2}{3}e$ particles should be $(\frac{2}{3})^2 = \frac{4}{9}$ in units of MIP's dE/dx. Therefore, an event which provides dE/dx smaller than that of a MIP could be a candidate $\frac{2}{3}e$ particle.

At the first step of the analysis, we selected events with a single downward-going, passing-through track which is fully contained inside the fiducial volume with restricted number of TOF hits, in order to reject albedo particles as well as the events interacted elastically in the BESS apparatus.

The MIP samples were selected by using the relation between rigidity, dE/dx in the upper and lower TOFs, and $1/\beta$ as shown by the heavy-line rectangles in Fig. 2. In further event selection, care must be exercised for those events

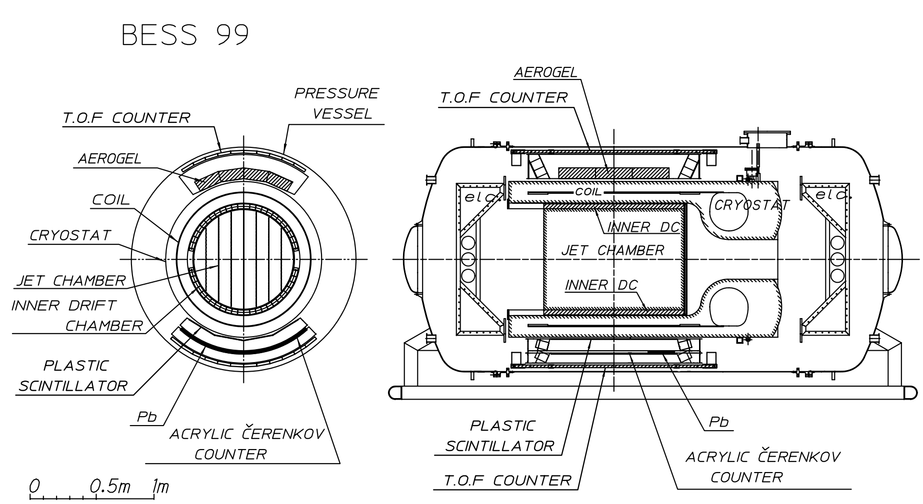

Fig. 1. Cross sectional view of the BESS spectrometer in its 1999 configuration.

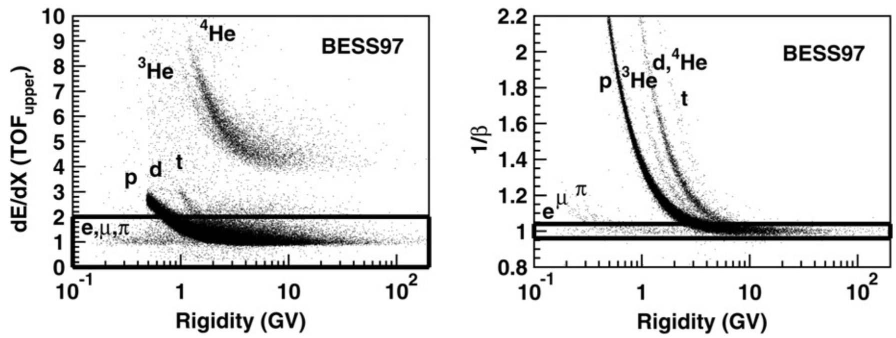

Fig. 2. Distributions of rigidity, dE/dx (upper TOF) and 1/β (BESS 1997). The heavy-line rectangles show selection boundaries for MIP samples.

whose track is not fully contained inside the TOF counter and may thus yield small dE/dx and "fake" $\frac{2}{3}e$ particles. At this step we also rejected those events that "grazed" the edge of the TOFs, by checking the intersection of the extrapolated chamber trajectory with the TOF position. The solid-line histogram in Fig. 3 shows the distribution of the distance, $|\Delta X|$, between this intersection and the center of the hit TOF counter paddle in the transverse, narrow, dimension. We fitted the error function to this $|\Delta X|$ histogram as shown by the dashed line in Fig. 3, and set the cut boundary for the $|\Delta X|$ as 4σ from the edge of TOF (dashed-dotted line). To confirm that this boundary is appropriate and effective to eliminate the "grazing" events, MIP events with dE/dx smaller than 0.7 were selected from the whole MIP samples. The dotted-line histogram in Fig. 3 shows the $|\Delta X|$ distribution of the MIP events with small dE/dx. Most of the events show $|\Delta X|$ larger than the cut boundary; that is, it was confirmed that this $|\Delta X|$ cut can eliminate the "grazing" events effectively.

At the second step, in order to eliminate backgrounds such as large-angle scattered events by ensuring good quality of R and β measurements, we applied several cuts on tracking and timing measurement quality parameters such as: (i) the number of used hits and the reduced χ^2 of the trajectory fitting, and (ii) the consistency between the JET track, hits in the IDCs, and the TOF timing information.

The solid-line histogram in Fig. 4 shows the dE/dx distribution of MIP samples which survived both of the first and second step selections. We fitted this solid-line histogram by the Landau function as shown by the dashed line in Fig. 4; this line is same as the dashed line in Fig. 5 ($Z = e$).

At the last step, we searched for the $\frac{2}{3}e$ particles. In order to identify the objects, the dE/dx distribution of $\frac{2}{3}e$ particles were estimated by scaling the Landau function for the MIP dE/dx obtained above (the number of photoelectrons for MIP is typically 500 at the center of TOF). As denoted by the solid line in Fig. 5, most of the expected dE/dx distribution of $\frac{2}{3}e$ particles is contained between the TOF trigger threshold (1/3 MIP) and the dE/dx distribution of MIP events. To keep high detection efficiency of $\frac{2}{3}e$ particles and minimize the probability to misidentify single-charged particles as the objects of our search, the selection boundary was set to 0.7 MIP. The selection efficiency is above 80% as shown by the integrated Landau function in Fig. 5.

Fig. 6 shows the distribution of dE/dx measured by the upper and lower TOFs in each flight. The events which yield either upper or lower TOF dE/dx smaller than 0.8

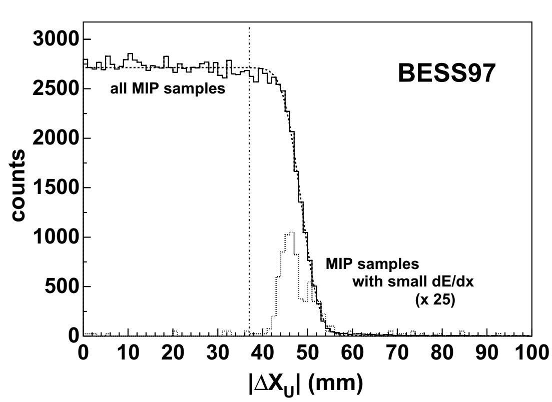

Fig. 3. The $|\Delta X|$ distribution of MIP samples (BESS 1997, upper TOF). The solid-line histogram represents the distribution of all MIP samples and is fitted by the error function shown by dashed line. The dotted-line histogram is the distribution of MIP samples with small dE/dx. The dashed-dotted line indicates the boundary of the cut.

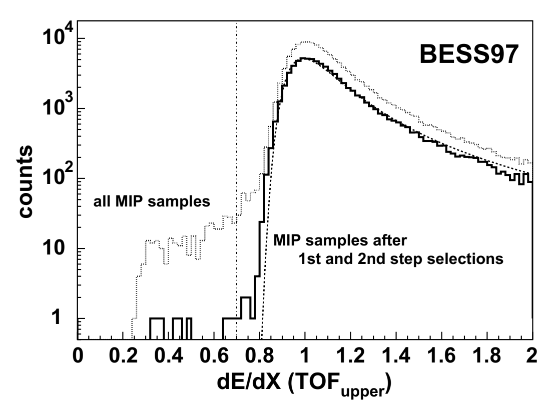

Fig. 4. The dE/dx distribution of MIP samples (BESS 1997, upper TOF). The dotted-line histogram is the distribution of all MIP samples without the first and the second step selections. The solid-line histogram is the distribution of MIP samples with the first and the second step selections. The dashed line is the Landau function fitted to the solid-line histogram. The dashed-dotted line shows the selection boundary of the search for $\frac{2}{3}e$ charged particles.

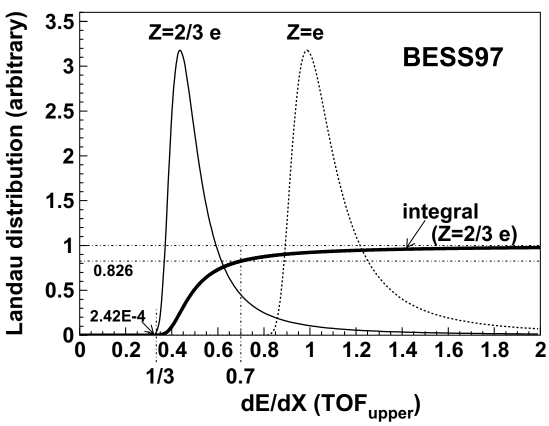

Fig. 5. The dE/dx distribution of $\frac{2}{3}e$ charged particles (thin solid line), which was estimated from the Landau function shown by the dashed line in Fig. 4. The integrated Landau function (thick solid line) denotes the detection efficiency.

are emphasized by large points. No event can be seen in the searched area which is defined as the region where both of dE/dx's are less than 0.7.

The large-pointed events are considered to be particles which scattered inside the BESS detector and "grazed" TOFs. These events cannot be quite eliminated by the first and second step selections in the present detector configuration. The number of these large-pointed events is consistent with the number estimated by a Monte Carlo simulation. According to the simulation, the probability that a particle is scattered both near upper and lower TOFs and grazed both the upper and lower TOFs is negligible with our event statistics.

5. Results

Since no $\frac{2}{3}e$ candidate was found, we calculated the resultant upper limit on the flux of cosmic-ray $\frac{2}{3}e$ particles, $\Phi_{\frac{2}{3}e}$, which is given by:

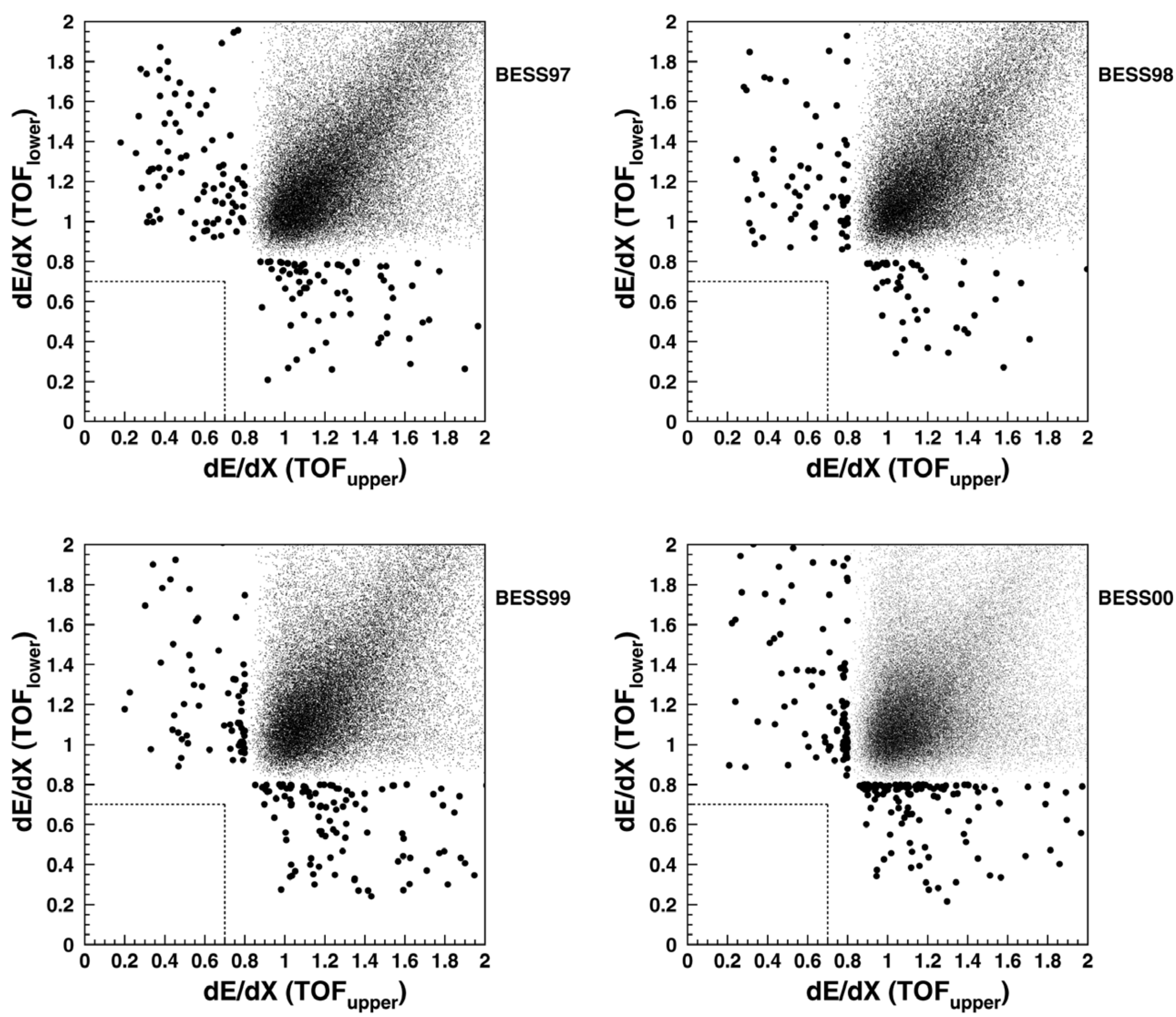

Fig. 6. Scatter plot of upper and lower dE/dx's for the each year's events which survived the first and the second step selections. No event can be found within the search region, which is defined as the region where both dE/dx's are less than 0.7 MIP. The events which yield either upper or lower dE/dx smaller than 0.8 are marked largely.

Table 2
The upper limits on the flux of cosmic-ray $\frac{2}{3}e$ charged particles for each four flights and their sum

Year	Upper limit (90% C.L.) $(\mathrm{cm}^2\ \mathrm{s\ sr})^{-1}$
1997 + 1998 + 1999 + 2000	4.5×10^{-7}
1997	3.0×10^{-6}
1998	2.9×10^{-6}
1999	2.1×10^{-6}
2000	9.6×10^{-7}

$$\Phi_{\frac{2}{3}e} \equiv \frac{N_{\mathrm{obs}}}{((S\Omega)\varepsilon_{\mathrm{total}}T_{\mathrm{live}})(1-\delta_{\mathrm{sys}})}. \quad (1)$$

The live time, T_{live}, was directly measured by a 1 MHz-clock pulse generator and scalers throughout the flights. As the number of the observed $\frac{2}{3}e$ particles, N_{obs}, we took 2.44 for the calculation of the 90% C.L. upper limit (Eidelman et al., 2004). We did not consider the effect of possible background contamination (Feldman and Cousins, 1998), because the amount of the background is negligibly small. In order to obtain the most conservative limit, the total systematic uncertainty, δ_{sys}, of ($S\Omega\ \varepsilon_{\mathrm{total}}T_{\mathrm{live}}$) was introduced, where $S\Omega$ is the geometrical acceptance, and $\varepsilon_{\mathrm{total}}$ is the total detection efficiency. The $\varepsilon_{\mathrm{total}}$ can be written as $\varepsilon_{\mathrm{total}} = \varepsilon_{\mathrm{trig}}\ \varepsilon_1\ \varepsilon_2\ \varepsilon_3\ \varepsilon_{\mathrm{acc}}\ \varepsilon_{\mathrm{air}}$. Since the mass and the energy of the fractionally charged particles are unknown, no energy dependency was taken into account. The efficiency of the first step selection (ε_1) and the survival probability in the residual atmosphere ($\varepsilon_{\mathrm{air}}$) were assumed to be 1. The effect of the $|\Delta X|$ cut was included in the calculation of $S\Omega$. The trigger efficiency ($\varepsilon_{\mathrm{trig}}$) was obtained by using detector beam-test data (Asaoka et al., 2002). The efficiency of the second step selection (ε_2) was estimated by using MIP samples. The efficiency of the third step selection (ε_3) was estimated using the Landau function described above. The probability of events without any hits or tracks caused by another accidental incident particle ($\varepsilon_{\mathrm{acc}}$) was derived from samples taken by the random trigger that was issued once a second throughout the flights. Typical values are: $\varepsilon_{\mathrm{trig}} \sim \frac{1}{60}$ ($\frac{1}{30}$ in 2000), $\varepsilon_2 \sim 90\%$, $\varepsilon_3 \sim 68\%$, $\varepsilon_{\mathrm{acc}} \sim 94\%$, and $S\Omega \sim 0.15\ \mathrm{m}^2$ sr. The systematic uncertainty was estimated to be $\delta_{\mathrm{sys}} \sim 4.6\%$, which includes the effect of minor variation among TOFs of the trigger threshold of $\frac{1}{3}$ MIP.

The resultant upper limit $\Phi_{\frac{2}{3}e}$ for 1997, 1998, 1999, 2000, and the integrated flight data were calculated to be 3.0×10^{-6}, 2.9×10^{-6}, 2.1×10^{-6}, 9.6×10^{-7}, and 4.5×10^{-7} $(\mathrm{cm}^2\ \mathrm{s\ sr})^{-1}$, respectively (Table 2).

6. Discussions and conclusion

We have searched for relativistic $\frac{2}{3}e$ charged particles in cosmic radiation with the BESS flight data obtained between 1997 and 2000. No candidate has been detected. We placed an upper limit of 4.5×10^{-7} $(\mathrm{cm}^2\ \mathrm{s\ sr})^{-1}$ (90% C.L.) on the flux of cosmic-ray $\frac{2}{3}e$ particles.

This upper limit is comparable to that obtained above the atmosphere by the AMS team (Sbarra et al., 2002) (see also Table 1). Although recent experiments on or under ground derive much more stringent results, as long as the penetration length of fractionally charged particles in the air is unknown, it is worthwhile using a balloon-borne platform. This environment is slightly different from that in free space because of the "thin target" of overlying atmosphere, so the experiment probes slightly different part of the possible phase space for fractionally charged particles.

We confirmed the ability of the BESS spectrometer to search for $\frac{2}{3}e$ particles, for the first time. More sensitive searches will be possible by combining other BESS flight data.

Acknowledgements

We thank NASA and the Columbia Scientific Balloon Facility (CSBF) for their professional and skillful work in carrying out the BESS flights. We also thank ISAS, KEK and ICEPP (the University of Tokyo) for their continuous support and encouragement for the BESS experiment. This experiment was supported by Grants-in-Aid, KAKENHI (9304033, 11440085, and 11694104) from the Ministry of Education, Culture, Sport, Science and Technology (MEXT), and by Heiwa Nakajima Foundation in Japan; and by NASA SR&T research grants in the USA.

References

Aglietta, M., Antonioli, P., Badino, G., et al. Search for fractionally charged particles in the Mont Blanc LSD scintillation detector. Astropart. Phys. 2, 29–34, 1994.

Ajima, Y., Anraku, K., Haga, T., et al. A superconducting solenoidal spectrometer for a balloon-borne experiment. Nucl. Instrum. Methods A 443, 71–100, 2000.

Ambrosio, M., Antolini, R., Baldini, A. et al. Final search for lightly ionizing particles with the MACRO detector, hep-ex/0402006, 2004.

Ambrosio, M., Antolini, R., Auriemma, G., et al. Search for lightly ionizing particles with the MACRO detector. Phys. Rev. D 62, 052003, 2000.

Asaoka, Y., Abe, K., Yoshimura, K., et al. Development of a large-area aerogel Cherenkov counter onboard BESS. Nucl. Instrum. Methods A 416, 236–242, 1998.

Asaoka, Y., Yoshimura, K., Yoshida, T., et al. Measurements of low-energy antiproton detection efficiency in BESS below 1 GeV. Nucl. Instrum. Methods A 489, 170–177, 2002.

DeLise, D.A., Bowen, T. Cosmic-ray search for fractionally charged particles. Phys. Rev. 140, B458–B462, 1965.

Eidelman, S., Hayes, K.G., Olive, K.A., et al. Particle data group. Phys. Lett. B, 592, 279–288, 2004.

Feldman, G.J., Cousins, R.D. Unified approach to the classical statistical analysis of small signals. Phys. Rev. D 57, 3873–3889, 1998.

Makida, Y., Anraku, K., Suzuki, J., et al. Ballooning of a thin superconducting solenoid for particle astrophysics. IEEE Trans. Appl. Supercon. 5, 658–661, 1995.

Mashimo, T., Orito, S., Kawagoe, K., et al. An underground search for anomalous penetrating particles such as massive magnetic monopoles. Phys. Lett. B 128, 327–332, 1983.

Kawagoe, K., Mashimo, T., Nakamura, S., et al. An underground search for fractionally charged penetrating particles. Lett. Nuovo Cimento 41, 604–608, 1984.

Mori, M., Oyama, Y., Suzuki, A., et al. Search for fractionally charged particles in Kamiokande II. Phys. Rev. D 43, 2843–2846, 1991.

Orito, S., Antiproton and antimatter: a balloon experiment with the model solenoid, KEK Report 87-19, in: Nishimura, J., Nakamura, K., Yamamoto, A. (Eds.), Proceedings of the ASTROMAG Workshop, pp. 111–123, 1987.

Sbarra, C., Casadei, D., Brocco, L. et al., Search for fractional charges in cosmic rays with AMS, Proc. 18th ECRS (Moscow), (astro-ph/0304192), 2002.

Shikaze, Y., Orito, S., Mitsui, T., et al. Large-area scintillator hodoscope with 50 ps timing resolution onboard BESS. Nucl. Instrum. Methods A 455, 596–606, 2000.

Yamamoto, A., Mito, T., Haruyama, T., et al. Conceptional design of a thin superconducting solenoid for particle astrophysics. IEEE Trans. Magn. 24, 1421–1424, 1988.